

INTERPRETATION OF HIGH RESOLUTION SAR DATA USING EXISTING GIS DATA IN URBAN AREAS

Timo Balz, Norbert Haala

Institute for Photogrammetry (ifp), University of Stuttgart, Germany
Geschwister-Scholl-Strasse 24D, D-70174 Stuttgart
Forename.Lastname@ifp.uni-stuttgart.de

KEY WORDS: SAR, Registration, Simulation, Georeferencing, GIS, Change Detection, Urban, Building

ABSTRACT:

Within the paper the automatic matching of existing GIS data to airborne SAR scenes for georeferencing is discussed. For this purpose simulated SAR images are generated based on the available GIS objects using a SAR simulator. These simulated scenes are matched against the captured SAR image in order to detect the given GIS objects in the SAR scene. The feasibility of the approach is demonstrated by the automatic localisation of street data, which have been captured originally for car navigation purposes. Since the horizontal accuracy of this data is limited, the georeferencing is further refined in a second step. This is realised by the automatic detection of landmark buildings, which are selected from a 3D city model. Since good initial values are available from the preceding localisation of the street regions, the matching problem can be solved despite the great complexity of SAR imagery if building objects are depicted. The high accuracy requirements, which can be met if the SAR scene is matched against a 3D city model, are for example required if a combination of the SAR scene with data from other sensors like optical images has to be realised. As it will be discussed in the final part of the paper, the presented matching process can in principle also be applied in order to detect inconsistencies between SAR scene and given GIS data. This will allow for potential applications in the context of change detection and update of the existing data.

1. INTRODUCTION

Due to the increasing geometric resolution of up to 10cm, which is provided from modern airborne SAR systems, large scale GIS-data collection seems to become feasible also for complex urban areas. Compared to optical images and LIDAR, airborne SAR is also advantageous for a number of remote sensing applications due to the range and weather independence of the image acquisition process. For these reasons, airborne SAR has the potential to become an alternative data base for the collection of 3D city models and road databases. However, problems result from the fact, that the interpretation of SAR imagery can become very complex for three-dimensionally structured scenes. Resulting from the run-time geometry and the side-looking property of SAR image acquisition, the evaluation of urban scenes is especially hindered by effects like occlusions, ambiguities or side-lobes. These problems for both automatic and manual approaches of SAR image interpretation are additionally aggravated by the growing amount of detail, which is provided from modern SAR systems. For data collection in urban areas, Digital Elevation Models (DEM) provided from InSAR can be used, alternatively (Soergel 2003), since the restriction to geometric information as it is provided from dense DEM can help to considerably simplify the required interpretation process. Nevertheless, in contrast to the application of airborne LIDAR, the INSAR based generation of very precise and reliable DEM in urban environments is still difficult.

For these reasons the initial collection of urban models is usually realised based on airborne LIDAR or optical imagery. In contrast, the rapid and area-covering data collection under all weather conditions, which is feasible by active systems using microwaves opts for the use of SAR-scenes especially for monitoring applications. For such scenarios, additional

information i.e. existing GIS data are usually already available. Thus, this information can be integrated in order to support the automatic evaluation and interpretation of SAR scenes. Within the paper this will be demonstrated by an approach aiming on an automatic matching of existing GIS data to airborne SAR. By these means an automatic geo-referencing of the SAR scene can be realized.

For our investigations images of the multifrequency polarimetric airborne SAR system DOSAR of the EADS Dornier GmbH are used (Hoffmann & Fischer 2002). The 3dB-resolution of the collected data is about 0.57m, the images were generated with a pixel resolution of 0.26m. In the first step, this SAR scene is mapped to an image simulated from a given street network in order to allow an automatic georeferencing (section 2). For this purpose, GDF data (Geographic Data File) are applied. GDF is European standard used to represent streets for car-navigation purposes. Since the horizontal accuracy of the street vectors is restricted to $\pm 3m$, the mapping accuracy of our process is limited to the same order of magnitude. Thus, further refinement is required. As it is discussed in section 3, this is realised by the detection of landmark buildings, which are selected from a 3D city model. These landmark buildings should have unique geometric properties in order to simplify the matching process. The matching is realised using a simulated SAR scene, which is generated from this building model using the sensor parameters of the real SAR system. The detection of corresponding elements between image and model is again based on the simulated and the real SAR image. Since good initial search areas are available from the localisation of the street network, the detection of the landmark buildings can be solved despite the increased complexity of the 3D object geometry.

If the SAR scene is matched against the 3D city model, high accuracy requirements of the georeferencing process can be met. This is for example required, if a combined evaluation of the SAR scene with other data sources like optical images or LIDAR is aspired. Up to now, SAR imagery is acquired in the so-called slant range geometry and then precisely geocorrected in a post-processing step. For this purpose frequently a Digital Terrain Model (DTM) is incorporated as an external reference surface. Since this reference surface does not represent objects like buildings, georeferencing errors are especially introduced in urban areas due to the height differences between the actual and the reference surface. This corresponds to effects like displacement or double mapping, which can be observed if ortho images are generated from optical imagery and a DTM in built-up areas. To avoid these effects, the generation of true-ortho images is based on a more detailed geometric representation provided from a 3D city model. If high-resolution SAR images are georeferenced, the availability of a correct reference surface is even more important due to the side-looking geometry of this type of sensor. This additionally votes for the integration of 3D building models for SAR image evaluation.

As it is discussed in section 4, inconsistencies or changes can be detected, if the 3D city model is matched against the real SAR image. Thus, our approach can in principle also be used as one part of an update process of existing 3D-city models, even though a considerable amount of research work is still required,

2. GEO-REFERENCING USING STREET NETWORK

The acquisition of airborne SAR imagery requires a direct measurement of sensor position and orientation with sufficient accuracy. By these means, the direct georeferencing of the SAR scene is already feasible. Nevertheless, this initial spatial reference is frequently not accurate enough for a number of applications. As an example, the initial reference of our test images had an offset of 150m. This spatial reference of the SAR image can be improved automatically using street vectors. In our application, the required GIS information is extracted from GDF (Geographical Data File) data, which is a European standard developed by organizations involved in the creation, update, supply and application of road network data. In Europe, the data are provided by the companies Navigation Technologies (NavTech) and TeleAtlas. While the primary focus of GDF data is on car navigation systems, it is frequently also used for applications like traffic analysis or fleet and dispatch management. The horizontal coordinates of the street vectors from GDF have an accuracy of 3m. Since height information is additionally required for our georeferencing process, the street vectors are overlaid to a given Digital Terrain Model and the vertical coordinates are extracted

Compared to the RADAR wavelength, streets have a smooth surface. For this reason, large portions of the incident radar energy are reflected away from the SAR sensor during image acquisition for this type of object. Usually, only a small part of the outgoing radar signal is redirected back towards the radar antenna. Thus, streets appear as dark regions in SAR images. In order to match the SAR image against the given street network dark regions within the SAR scene are applied. As a first step, the GDF data are first approximately mapped to the SAR image based on the available transformation from direct georeferencing. The GDF street vectors are then transformed to a binary image in order to allow for a pixel based matching between this image and the SAR scene. By these means the exact transformation between the SAR scene and the GDF data

is determined. The relatively time-consuming matching process is sped up by a coarse-to-fine strategy. Therefore, the original image resolution of 0.26m is reduced in the first step, and the matching result is refined with the original resolution in the second step.



Figure 1: Matching result between a DOSAR image and GDF-streets in urban areas.

The matching is realised for search areas of a 0.24km^2 size, which are extracted from both the GDF data and the SAR scene. For visualisation purposes, in Figure 1 the binarized GDF-street data were overlaid to the respective SAR image section after the matching process. The good correspondences, which can be achieved for search areas in an urban environment are clearly visible.

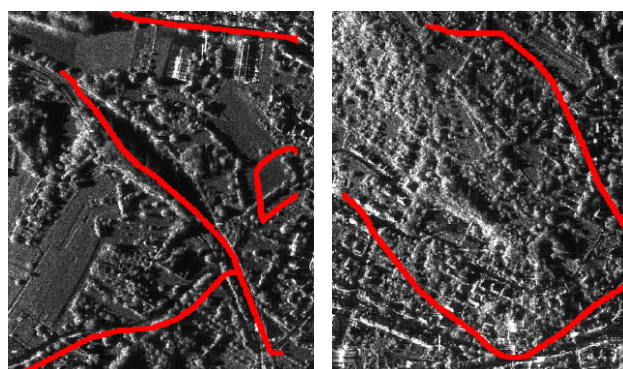


Figure 2: Erroneously detected correspondences

Nevertheless, problems can occur for the matching process, if only a small amount of streets and junctions is available. These problems, which mainly occur in rural regions are further aggravated if there is only slight contrast between the streets and the surrounding areas. Two examples for such erroneous matching results are given in Figure 2.



Figure 3: Footprint of the SAR image and the search areas

In order to avoid such errors, search areas should contain a sufficient number of streets and junctions. For this reason, suitable search areas should be provided, which allow for a stable and error free matching process. This is realised by an automated search method prior to the matching process. In this step, the given street network is analysed to extract a sufficient number of search areas, which are evenly distributed over the complete SAR scene. In Figure 3 the footprints of the SAR image sections (grey area) used in our investigations are overlaid to the GDF-data (green lines). The automatically

selected search areas are represented by the red points. Despite the discussed criterion, these search areas are not very well distributed. This results from the fact that a sufficient number of streets and junctions can only be found in city regions. Even worse, due to the small swath-width of the image, the points are unfavourable distributed approximately on one line. Nevertheless, in our experiments the amount of corresponding search areas is sufficient to automatically detect wrong matches and to compute the required transformation parameters by a robust estimation.

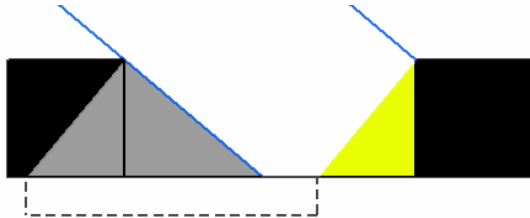


Figure 4: Supposed street position, shifted in near range direction

One factor limiting the accuracy of the matching process is the quality of the available street vectors. Smaller errors can also result from reflecting objects on or near the street like cars or signs. Even larger systematic errors can occur especially in urban areas from buildings at or near the streets. As it is depicted in Figure 4, a combination of shadow and layover effects can result in a shift of the detected street position in the near range direction. Assuming a building height of 10m and an off-nadir angle of 70°, the shift is approximately 3.6m. In our experiments, this effect limits the overall accuracy for the coregistration of the SAR image and the GDF street map to 6m. Thus, for a number of applications the accuracy has to be further increased using a more detailed three-dimensional model of the environment.

3. GEOREFERENCING USING 3D BUILDING MODELS

In our approach, the georeferencing process is refined by a 3D city model. These city models are frequently collected from aerial images or airborne LIDAR at accuracies in the decimetre level, but in contrast to the GDF-street data they are not available for all areas. Still the growing popularity of city models for task like visualisation and simulation will definitely stimulate the further spread of this type of data.

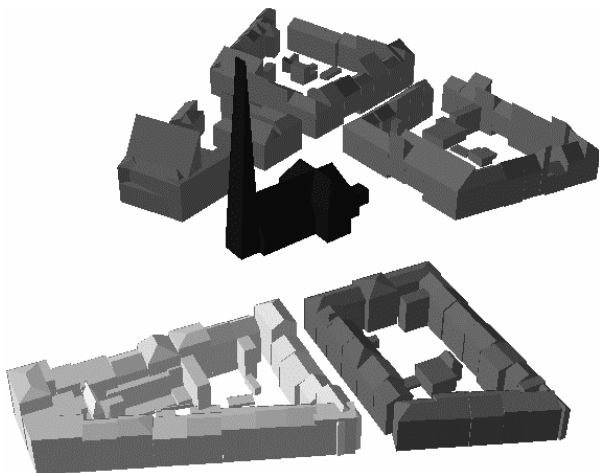


Figure 5: Subset of the 3D-city model of Karlsruhe.

For our investigations a 3D city model of Karlsruhe is used, which was generated using LIDAR DEM in combination with given outlines of the buildings (Haala & Brenner 1999). A subset of this data set is depicted in Figure 5.

3.1 SAR simulation

Similar to the localisation of the street networks, the georeferencing from 3D building models uses simulated SAR images. While the street vectors could be transformed to a binary image relatively easily, for complex 3D data like city models a more advanced SAR simulator is required. This simulator has to be especially adapted for urban environments since this is different from the simulation of natural environments due to the different backscattering behaviours (Franceschetti et al 2003). These SAR simulators are frequently used as a key tool for the analysis and interpretation of SAR data (Leberl & Bolter 2001). Since the complex interaction of different SAR effects is very difficult to understand even for experienced human operators, SAR simulators are also used for training purposes. Additionally, SAR simulations are applied during mission planning especially in dense urban environments to avoid occluded areas (Soergel et al 2003).

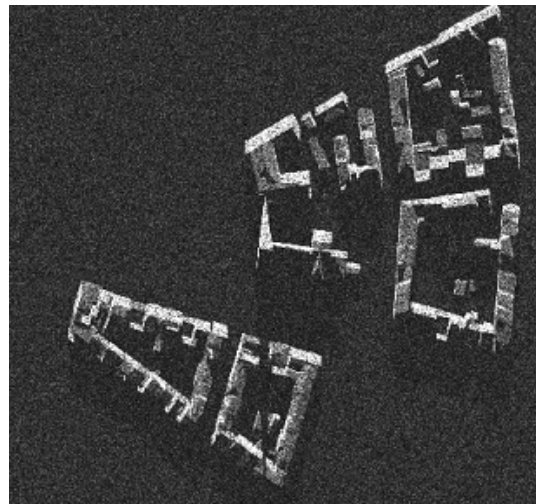


Figure 6: Simulated SAR image of the test area.

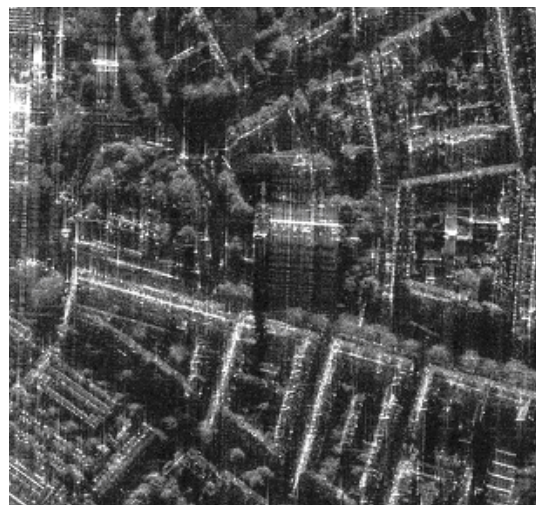


Figure 7: DOSAR image of the test area.

The simulated image depicted in Figure 6 was generated using the SAR View Light (basis version) simulator from EADS Deutschland GmbH. The required input data were provided

from the 3D model shown in Figure 5, while parameters like flight direction and off-nadir angle were set according to the real scene to be analysed

This real DOSAR image, which was collected at an off-nadir angle of 70° is depicted in Figure 7. One reason for the differences to the simulated SAR image in Figure 6 is that for the simulation process only building models were used, no information on additional objects like trees was integrated. Since the used city models depicted in Figure 5 is a generalized and simplified representation of the reality, these differences to the reality will always result in incomplete and erroneous simulation results. Additionally, a correct simulation of the backscattering characteristics would require the specification of the respective physical properties for the different objects surfaces. However, individual characteristics such as surface roughness, conductivity or permeability were not used in our investigations. However, the consistency between the simulated and the real image still allowed for the aspired matching.

3.2 Selection of landmark buildings

This matching process can be simplified, if buildings with unique geometric properties are used. These landmark buildings only have to be 'unique' in a local area. The size of this search area of approximately $\pm 6\text{-}\pm 10\text{m}$ corresponds to the accuracy of the initial georeferencing based on the GDF-data. The selected landmark buildings should also be separated from the neighbouring buildings to avoid problems due to occlusions.

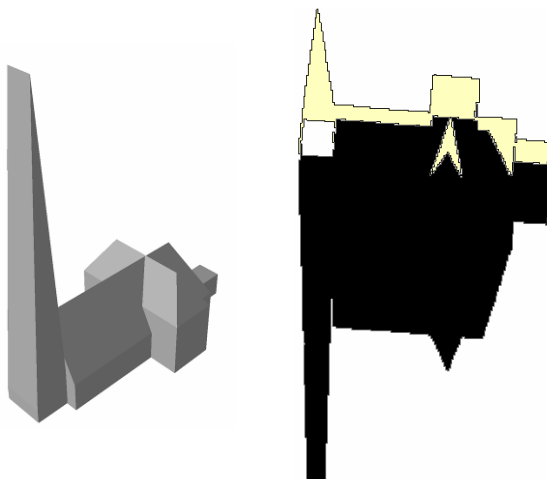


Figure 8: 3D Model of the St. Bernhardus church (left) and SAR simulation as vector representation (right)

For our experiments the 3D model of the St. Bernhardus church, depicted in the left image of Figure 8 was selected manually. Based on the parameters of the real flight, the simulated image depicted on the right side of Figure 8 is generated. The simulation without any speckle effects allows for reliable segmentation of the image, which results in a vector representation consisting of bright and shadow areas. This vector representation is advantageous, especially if large areas have to be handled within multi-scale approaches. In a second preprocessing step, vector polygons are also extracted on multiple pyramid levels from the real SAR image using an adaptive threshold approach (Levine & Shaheen 1981).

3.3 Matching

Our matching is based on analysing the size of bright regions within the simulated and the real image. Starting with the coarsest level, corresponding regions are searched within the

different pyramid levels in a coarse-to-fine-approach, which reduces the overall number of polygons to be matched and cuts down the error rate for the process. In the largest image scale, the segmentation of the real SAR scene depicted in Figure 7 results in 40505 regions. Within the matching, three potential correspondences, i.e. possible positions of the simulated image in the real image are detected. Only the correct match fits to the potential positions of the landmark as it is determined from initial georeferencing using the street network. In a second step, the exact position of the landmark is provided from a correlation based pixel-by-pixel analysis.

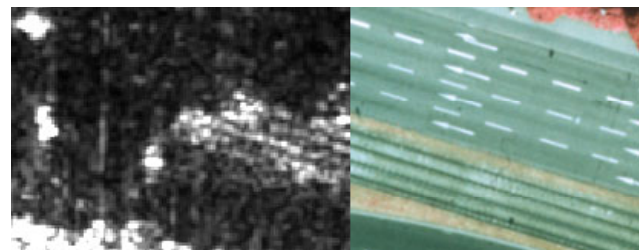


Figure 9: DOSAR image (left) and orthoimage (right)

The accuracy of the geo-referencing process is demonstrated in Figure 9. It depicts a small area in the vicinity of the landmark used for the matching process. On the left side, the image contains a section of the automatically geo-referenced SAR image. This is stitched to an orthoimage on the right, which was generated from an aerial image. The good co-registration and geo-referencing of both data sets is e.g. indicated by the rails, which fits well against each other in both images. Despite these visual clues, the exact determination of our georeferencing accuracy is difficult, since the detection of corresponding points, which are suitable for measurement is problematic even for an experienced operator. We estimated an accuracy of 1.5m in the vicinity of the church for our automatic approach, which is equivalent to 6 pixel of the image or 3 times the 3-dB resolution of the SAR system. In our opinion, this is comparable to a manual referencing for this type of scene.

4. DATA FUSION

The combination of an exactly georeferenced SAR image with an optical images can for example be used within an integrated classification or segmentation process. Additionally, the coregistration between the SAR image and the available GIS-data can in principle be used to detect inconsistencies by a modified matching process. Within this section some first steps towards such a very complex process are discussed.

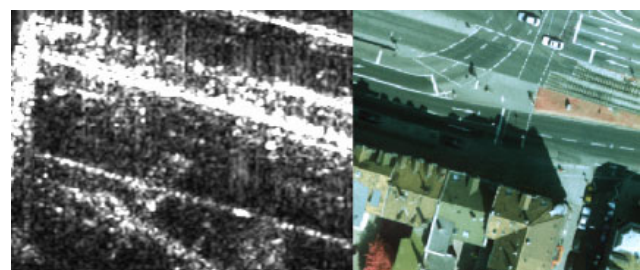


Figure 10: DOSAR image (left) and orthoimage (right)

4.1 Registration of SAR and optical imagery in urban areas

As it is demonstrated in Figure 9 a good fit between the georeferenced SAR scene and the ortho image is feasible, if the terrain surface is depicted. Figure 10 gives another example in

the vicinity of the matched landmark. Again, the left part contains the georeferenced SAR image, while the right part shows a section of the ortho image. In contrast to Figure 9 within this example buildings are present, which results in considerable differences between SAR and optical image. As an example within the SAR image of Figure 10, the vertical walls result the bright areas in front of the buildings. In contrast, for the true-ortho image on the right, the position of the building roofs exactly corresponds to the position of the building footprints.

Some of effects, which occur if a single building is depicted in a SAR image are depicted in Figure 11. The areas *A* and *F* are not influenced by the building geometry, thus these reflectance values provide surface information for the surrounding area. In principle these areas can be directly combined with optical imagery i.e. to improve a land-use classification. In contrast, due to effects like layover and shadow the areas *B*, *C*, *D* and *E* are directly affected by the building. These image regions can for example be applied to control the validity of the building if this is available. As an example, the length of bright areas in range can help to measure the height of the building object (Kirscht & Rinke 1998).

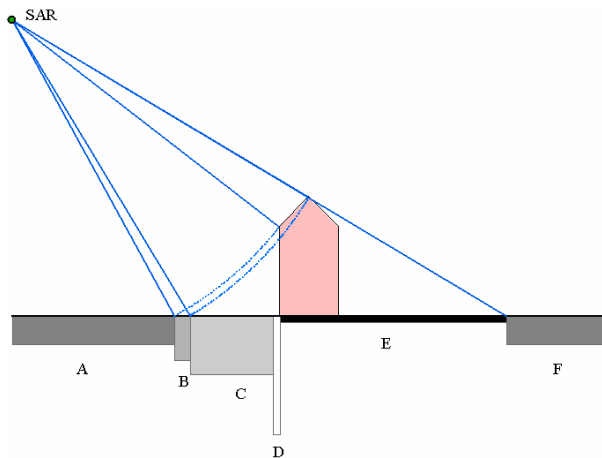


Figure 11: Areas depicted in the vicinity of a building depending on SAR geometry

4.2 Detection of inconsistencies

In order to discuss the potential, but also the problems of our matching process in the context of change detection applications, a smaller section of the 3D city model is analysed in more detail.

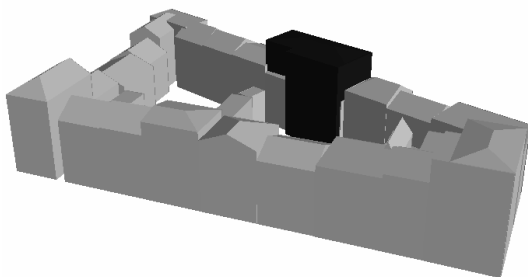


Figure 12: Manipulated 3D-model

The building block, which is used for this purpose is depicted in Figure 12. Within this block, the original geometry of the black building was changed manually. In the ideal case, this erroneous part of the block should be detected by a model to

image matching process. Similar to the georeferencing process, a SAR image is simulated based on this model as a first processing step.

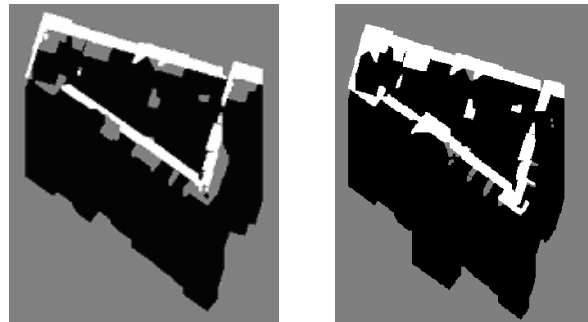


Figure 13: Simulated image of the original 3D-model (left) and of the modified 3D-model (right)

Figure 13 depicts the result of the SAR simulation process for the original model on the left, while the simulation for the manipulated 3D model is shown on the right. In contrast to the georeferencing process discussed in section 3, the coregistration of the simulated image in Figure 13 to the real SAR scene is already available. This allows for a direct comparison between both datasets.

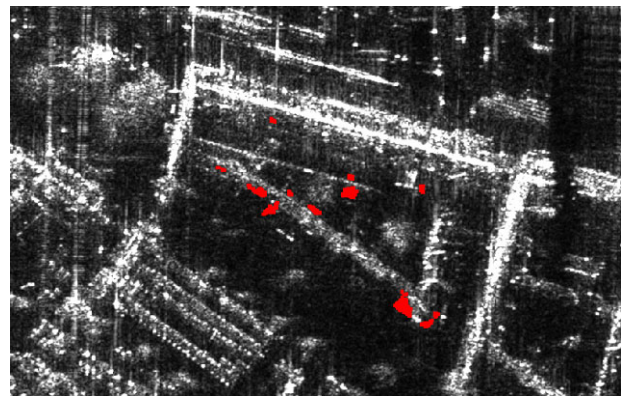


Figure 14: Detected changes of the building block overlaying a DOSAR image

The discrepancies between the real SAR scene and the simulated image, which was generated based on the manipulated 3D model are shown in Figure 14. For visualisation purposes, the automatically detected inconsistencies are overlaid as red areas to the SAR image. These differences were detected based on a comparison of the bright regions, which are generated from layover effects.

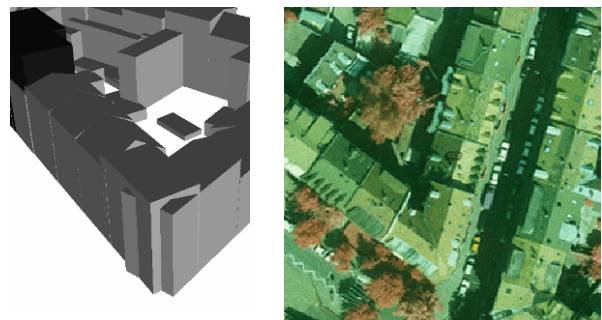


Figure 15: Section of the available 3D-model (left) and corresponding ortho image (right).

Obviously, the detected differences between the 3D model and image are not restricted to the manipulated building. Some

differences occur inside the building block, additional differences between model and SAR image are detected in the south-east corner of the image. This part of the 3D building block model is depicted on the left side of Figure 15. In order to allow for a visual comparison between the available 3D model and the reality, the corresponding section of the ortho image is depicted additionally in the right part of Figure 15. A number of deviations, which are due to errors or simplifications of the 3D model generation process are clearly visible. Unfortunately, these effects can occur for every city model, making it difficult to use this data as ground truth for any automatic change detection approach.

5. CONCLUSION

Airborne SAR systems allow for image collection, which is independent from daytime and weather conditions. The increasing geometric resolution, which is available from current systems offers the opportunity to use this technology also for data collection in built-up areas. However, in these regions the oblique SAR illumination limits the visibility of objects and hinders the image interpretation for example due to inherent artefacts. Thus, additional information as it is provided by GIS should be integrated in order to support the analysis of SAR data.

Within the paper, this was demonstrated by an approach for the georeferencing of SAR scenes based on given street networks and 3D city models. The use of such 3D models for SAR processing is also required for the integration of SAR scenes with additional data like optical images, i.e. to allow a combined classification. This can only be realised, if the precise coregistration of the different sensor data is feasible on the pixel level. For high resolution imagery in urban areas, this requires an orthorectification of the SAR scene using a reference surface, which contains objects like buildings. Thus, a 3D city model has to be available in addition to the terrain surface also for this type of application.

In principle, the matching of SAR scenes, which are simulated from available 3D models against real SAR images can also be applied for change detection purposes by controlling the validity of the used 3D GIS data. Current problems to be solved for such a matching process result from the fact, that the influence of vegetation, which is usually not represented in a 3D city model can not be neglected. Frequently, detailed information on the surface material of objects is also not available. Other problems occur since the geometry of the available 3D building models is only a simplified representation of the reality and thus requires a reliable evaluation of the detected differences.

6. ACKNOWLEDGEMENTS

We thank the EADS Deutschland GmbH for providing us with the simulated and real SAR data and for their help in making this work possible.

7. REFERENCE LIST

Franceschetti, G., Iodice, A., Riccio, D. & Ruello, G. [2003]. SAR Raw Signal Simulation for Urban Structures. *IEEE Transactions on Geoscience and Remote Sensing* **41**(9), pp.1986-1995.

Haala, N. & Brenner, C. [1999]. Extraction of buildings and trees in urban environments. *ISPRS Journal of Photogrammetry & Remote Sensing* **54**(2-3), pp.130-137.

Hoffmann, K. & Fischer, P. [2002]. DOSAR: A Multifrequency Polarimetric and Interferometric Airborne SAR-System. Geoscience and Remote Sensing Symposium, 2002. IGARSS '02., pp.1708-1710.

Kirscht, M. & Rinke, K. [1998]. 3D Reconstruction of Buildings and Vegetation from Synthetic Aperture Radar (SAR) images. IAPR Workshop on Machine Vision Applications, pp.228-231.

Leberl, F. & Bolter, R. [2001]. Building reconstruction from Synthetic Aperture Radar images and interferometry. Automatic Extraction of Man-Made Objects From Aerial and Space Images (III).

Levine, M.D. & Shaheen, S.I. [1981]. A Modular Computer Vision System for Picture Segmentation and Interpretation. *IEEE Transactions on Pattern Analysis and Machine Intelligence* **3**(5), pp.540-556.

Soergel, U. [2003] Iterative Verfahren zur Detektion und Rekonstruktion von Gebäuden in SAR- und InSAR-Daten . University of Hannover.

Soergel, U., Schulz, K., Thoennessen, U. & Stilla, U. [2003]. Event-driven SAR Data Acquisition in Urban Areas Using GIS. *GIS* **16**(12)